CHIN. PHYS. LETT. Vol. 34, No. 10 (2017) 100501

Localized Optical Waves in Defocusing Regime of Negative-Index Materials *

Wen-Hao Xu(许文昊)[1,2], Zhan-Ying Yang(杨战营)[1,2**], Chong Liu(刘冲)[1,2**], Wen-Li Yang(杨文力)[2,3]
[1]School of Physics, Northwest University, Xi'an 710069
[2]Shaanxi Key Laboratory for Theoretical Physics Frontiers, Xi'an 710069
[3]Institute of Modern Physics, Northwest University, Xi'an 710069

(Received 8 May 2017)

We study optical localized waves on a plane-wave background in negative-index materials governed by the defocusing nonlinear Schrödinger equation with self-steepening effect. Important characteristics of localized waves, such as the excitations, transitions, propagation stability, and mechanism, are revealed in detail. An intriguing sequential transition that involves the rogue wave, antidark–dark soliton pair, antidark soliton and antidark soliton pair can be triggered as the self-steepening effect attenuates. The corresponding phase diagram is established in the defocusing regime of negative-index materials. The propagation stability of the localized waves is confirmed numerically. In particular, our results illuminate the transition mechanism by establishing the exact correspondence between the transition and the modulation instability analysis.

PACS: 05.45.Yv, 41.20.Jb, 42.65.−k, 78.20.Bh DOI: 10.1088/0256-307X/34/10/100501

Metamaterials are artificial structures that have peculiar properties which are absent in naturally occurring materials. One of the most notable metamaterials is the negative-index material (NIM) with simultaneously negative electric and magnetic responses, which was originally postulated theoretically by Veselago[1] and now offers exciting new prospects for manipulating light.[2,3] In nonlinear optics, the development[4–6] of NIMs has inspired extensive research on several nonlinear optical phenomena that can occur in NIMs because of the change in the sign of the refractive index in both the spatial and frequency domains.[7] In particular, significant progress has been made recently on the nonlinear properties of optical wave propagation in NIMs, including the formation of localized waves, harmonic generation, and modulation instability (MI).[8–10] It is found that the unusual properties of NIMs results, for example, in some new classes of solitons that cannot exist in positive-index materials.[11] Correspondingly, the bright and dark solitons have been experimentally demonstrated in NIMs based on the standard nonlinear Schrödinger equation (NLSE).[12]

Recently, especial attention has been paid to the ultrashort pulse propagation in NIMs. It is demonstrated that the dynamics of ultrashort pulses in NIMs without nonlinear magnetization can be described by a generalized NLSE.[13] The latter thus describes ultrashort pulses in NIMs with higher accuracy than the standard NLSE. Different types of soliton including bright, dark, and combined solitary-wave structures have been analytically or numerically demonstrated.[14–17]

In addition to the solitons, localized waves on a plane-wave background have recently been the subject of intensive investigations in nonlinear optics.[18–26] Generally, localized waves riding on a plane-wave background exhibit the onset of MI, which are known as rogue waves and breathers.[27,28] In contrast to the soliton with stable structural feature, breathers and rogue waves are localized structures with an unstable characteristic. Breathers are the localized breathing waves with a periodic profile in a certain direction, and rogue waves are rare, short-lived, and localized in both space and time.[29–32] Recently, rogue waves and breathers have been explored in the transmission line analogue of a nonlinear NIM[33] based on the standard NLSE. Moreover, characteristics of rogue waves and breathers in the nonlinear NIM with cubic-quintic nonlinearities have been studied.[34] So far, most properties of the generation of rogue waves and breathers in NIMs have been studied in the focusing regime. The characteristics of rogue waves in the defocusing regime of NIMs remain essentially unexplored.

In this work, we study ultrashort pulse propagation in the defocusing regime of NIMs with self-steepening effect which is governed by a modified NLSE presented in Ref. [35]. It should be pointed out that the role of self-steepening effect in MI and the propagation property of standard bright soliton in NIM have been studied.[36,37] However, the important characteristics of optical rogue waves and solitons on a plane-wave background in NIM have not been studied, not only the properties of rogue-wave and soliton excitations but also the transitions and mechanism have not even been analyzed completely. Here we focus our attention on important characteristics of localized waves, i.e., the excitation, transition, propagation stability, and mechanism. We reveal that an intriguing sequential transition involving the rogue wave, antidark–dark soliton pair, antidark soliton, and antidark soliton pair can be triggered as the self-steepening effect attenuates. The corresponding phase diagram is established and the propagation

*Supported by the National Natural Science Foundation of China under Grant Nos 11475135, 11547302, 11434013 and 11425522.
**Corresponding author. Email: zyyang@nwu.edu.cn; chongliu@nwu.edu.cn
© 2017 Chinese Physical Society and IOP Publishing Ltd

stability is confirmed numerically. In particular, our results illuminate the transition mechanism by establishing the exact correspondence between the transition and the modulation instability analysis.

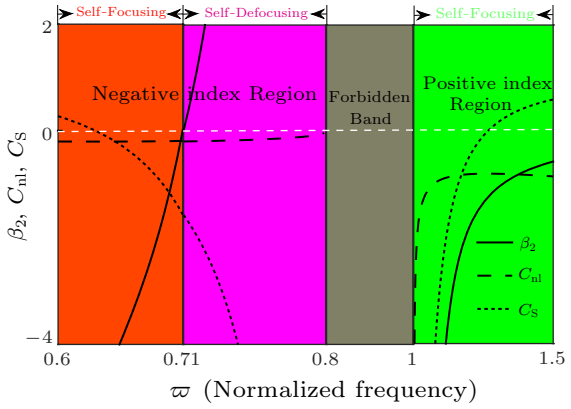

Fig. 1. Phase regions of metamaterial divided by variations of β_2, $C_{\rm nl}$, $C_{\rm s}$ (Eq. (3)) versus $\varpi(=\omega/\omega_{\rm pe})$ with $\omega_{\rm pm}/\omega_{\rm pe}=0.8$. Here β_2 and $C_{\rm nl}$ are calculated in units of $1/c\omega$ and $\chi^3\omega/(2c)$, respectively.

From the Maxwell equations, the wave equation for the pulse propagation in uniform, lossless medium under the condition of nonlinear polarization is given as

$$\frac{\partial^2 E(z,t)}{\partial z^2}=\mu(\omega)\epsilon(\omega)\frac{\partial^2 E(z,t)}{\partial t^2}+\mu(\omega)\frac{\partial^2 P_{\rm nl}(z,t)}{\partial t^2},\quad(1)$$

where the electric field $E(z,t)$ propagates along the z direction, the nonlinear polarization $P_{\rm nl}(z,t)$ satisfies the Kerr nonlinearity $P_{\rm nl}=\epsilon\chi^3|E|^2E$, and χ^3 represents the third-order susceptibilities. For an ideal lossless metamaterial, the electric permittivity and magnetic permeability can be described by the Drude model $\epsilon_{\rm r}(\omega)=(1-\omega_{\rm pe}^2/\omega^2)$, $\mu_{\rm r}(\omega)=(1-\omega_{\rm pm}^2/\omega^2)$, where $\omega_{\rm pe}$ and $\omega_{\rm pm}$ are the electric and magnetic plasma frequencies, respectively. Therefore, the refractive index is $n(\omega)=\sqrt{1-\omega_{\rm pe}^2/\omega^2}\sqrt{1-\omega_{\rm pm}^2/\omega^2}$. Generally, we can induce an envelope for the electric field in the form $E(z,t)=\frac{1}{2}A(z,t)\exp(ikz-i\omega t)$, where $A(z,t)$ is the amplitude of electric field, $k=n(\omega)\omega/c$ is the wave number at the carrier frequency ω, n is the refractive index at ω, and c represents the velocity of light. Following the procedure described in Refs. [13,35], the higher-order NLSE with self-steepening effect which describes the ultrashort pulse propagation in the NIM can be written as

$$i\frac{\partial A}{\partial\xi}+\frac{\beta_2}{2}\frac{\partial^2 A}{\partial\tau^2}+C_{\rm nl}\Big(1+i\frac{C_{\rm s}}{\omega}\frac{\partial}{\partial\tau}\Big)|A|^2A=0,\quad(2)$$

where $\xi=z$, and $\tau=t-z/V_{\rm g}$ with the group velocity $V_{\rm g}=\frac{d\omega}{dk}$. Real parameters β_2, $C_{\rm nl}$, $C_{\rm s}$ are the group velocity dispersion, nonlinearity, and self-steepening coefficients, respectively, which are given by

$$\begin{aligned}\beta_2&=\frac{1}{cn\omega}\Big(1+\frac{3\omega_{\rm pe}^2\omega_{\rm pm}^2}{\omega^4}\Big)-\frac{1}{cn^3\omega}\Big(1-\frac{\omega_{\rm pe}^2\omega_{\rm pm}^2}{\omega^4}\Big),\\ C_{\rm nl}&=\frac{\chi^3\omega}{2nc}\Big(\frac{\omega_{\rm pm}^2}{\omega^2}-1\Big),\\ C_{\rm s}&=1+\frac{\omega_{\rm pe}^2\omega_{\rm pm}^2-\omega^4}{n^2\omega^4}-\frac{\omega^2+\omega_{\rm pm}^2}{\omega_{\rm pm}^2-\omega^2}.\end{aligned}\quad(3)$$

The property of the parameterized β_2, $C_{\rm nl}$, $C_{\rm s}$ given by Eq. (3) plays a key role in the characteristic of metamaterials. Indeed, we find that there exist some different regions of metamaterials divided by variations of β_2, $C_{\rm nl}$, $C_{\rm s}$ versus the introduced normalized frequency $\varpi=\omega/\omega_{\rm pe}$. Specifically, (i) in the frequency interval $\omega_{\rm pm}/\omega_{\rm pe}<\varpi<1$, implying $\epsilon_{\rm r}(\varpi)<0$ and $\mu_{\rm r}(\varpi)>0$, the electromagnetic wave in this particular case is evanescent with a complex index. This corresponds to the forbidden band. (ii) When $\varpi<\omega_{\rm pm}/\omega_{\rm pe}$, thus $\epsilon_{\rm r}(\varpi)<0$, $\mu_{\rm r}(\varpi)<0$, we obtain the negative index region. (iii) In the rest case $\varpi>1$, indicating $\epsilon_{\rm r}(\varpi)>0$, $\mu_{\rm r}(\varpi)>0$, the positive index region of metamaterials is obtained.

Figure 1 displays the characteristics of β_2, $C_{\rm nl}$, $C_{\rm s}$ versus the normalized frequency ϖ with $\omega_{\rm pm}/\omega_{\rm pe}=0.8$. Here β_2 and $C_{\rm nl}$ are calculated in units of $1/c\omega$ and $\chi^3\omega/2c$, respectively. It is evident that in the positive index region ($\varpi>1$), only the self-focusing regime ($\beta_2<0$, $C_{\rm nl}<0$) exists. In contrast, in the negative index region, both self-focusing and self-defocusing regimes can exist. This stems from the fact that the dispersion β_2 can be either positive or negative, while the nonlinearity $C_{\rm nl}$ is always negative. Depending on the critical frequency at the zero point of β_2, i.e., $\varpi\approx0.71$, we distinguish the self-focusing ($0<\varpi<0.71$) and self-defocusing regime ($0.71<\varpi<0.8$) in the negative refractive index region.

Note that the role of the self-steepening effect in modulation instability in NIMs in Eq. (2) has been studied.[37] It is demonstrated numerically that the negative self-steepening effect moves the center of generated bright soliton toward the leading side, and shifts a part of energy of the generated soliton toward the red side.[35] Recently, the propagation property of standard bright soliton in Eq. (2) has been studied by exact soliton solutions.[38] However, to our knowledge, the important characteristics of localized wave on a plane-wave background in NIM in Eq. (2) have not been studied, not only the properties of localized-wave transitions but also the physical mechanisms have not even been analyzed completely. On the other hand, the rogue wave excitations and the transitions between rogue waves and solitons in the focusing regime have been demonstrated in many nonlinear physical systems.[20–26] However, less attention has been paid to analyzing transition properties and the physical mechanism in the defocusing regime. Thus we study the localized-wave excitations and the physical mech-

anism in the defocusing regime of NIMs in Eq. (2).

To this end, we introduce the normalized variables $T = \tau/\tau_{\rm p}, Z = \xi/2l_{\rm d}$, where $\tau_{\rm p}$ is the width of the input pulse, $l_{\rm d} = \tau_{\rm p}^2/|\beta_2|$ is the dispersion length, $l_{\rm nl} = 1/(|C_{\rm nl}|A_0^2)$ is the nonlinear length, and $U = A/\sqrt{P_0}$ is the power of the input field $\sqrt{P_0}$. As a result, ultrashort pulse propagation in defocusing regime ($0.71 < \varpi < 0.8$) of NIM in Eq. (2) is written as

$$i\frac{\partial U}{\partial Z} + \frac{\partial^2 U}{\partial T^2} - g|U|^2U + iS\frac{\partial}{\partial T}(|U|^2U) = 0. \quad (4)$$

The nonlinear parameter $g = 2l_{\rm d}/l_{\rm nl}$ and the self-steepening parameter $S = g|C_{\rm s}|/\tau_{\rm p}\omega$ are positive constants, where $\omega = 2\pi/\tau_{\rm opt}$ and $\tau_{\rm opt}$ are the optical periods.

Using the Darboux transformation described in Ref. [20], a general exact rational solution on a plane-wave background in the defocusing regime of NIM, Eq. (6), is given by

$$U(T,Z) = U_0\left\{\frac{2m(T-\nu_2 Z) - i[3+\Theta(T,Z)]}{2im(T-\nu_1 Z) + i[1-\Theta(T,Z)]}\right\}, \quad (5)$$

where $U_0 = ae^{i\theta}$, $\theta = qT - (m\alpha + q^2)Z$ denotes the plane-wave background with the amplitude a and frequency q, and $\Theta(T,Z) = 2m\alpha(T-\mu_1 Z)(T-\mu_2 Z)$. One should note that, in contrast to the rational solution describing the prototype of rogue waves,[18] Eq. (7) is a rational solution with multiple velocities ν_1, ν_2, μ_1, μ_2, and S,

$$\nu_1 = 2q + 3m, \quad \nu_2 = (\nu_1 + 4\alpha), \quad (6)$$

$$\mu_1 = 2(q+m) + \sqrt{m(m+2\alpha)}, \quad (7)$$

$$\mu_2 = 2(q+m) - \sqrt{m(m+2\alpha)}, \quad (8)$$

$$S = \frac{g}{2\pi\frac{\tau_{\rm p}}{\tau_{\rm opt}}}\left|\frac{0.64 - 2\varpi^2 + \varpi^4}{0.64 - 1.64\varpi^2 + \varpi^4}\right|, \quad (9)$$

where $m = a^2 S(>0)$ and $\alpha = (g/S + q)$. For special parameter values $a = 1$ and $q = -1$, this solution reduces to the simplest solution obtained in Ref. [20].

In general, a localized wave solution formed by a nonlinear superposition of rational function on a plane-wave background can be used to describe the prototype of rogue wave phenomena,[39] which is known as the rogue wave solution. In the case of the standard NLSE, the rogue wave solution possesses a velocity induced by the background frequency. This velocity has no impact on the property of rogue waves since it can be overlooked by the Galilean transformation. In the case of the NLSE with higher-order effects, the rogue wave solution possesses a velocity arising from the higher-order effects. This velocity is nontrivial, since it can induce the transition from rogue waves to W-shaped solitons.[22] However, the rational solution (7) has multiple velocities ν_1, ν_2, μ_1 and μ_2. Thus we expect the interesting properties of localized waves described by Eq. (7). Indeed, we find that the multiple velocities ν_1, ν_2, μ_1 and μ_2 play a key role in the types of localized waves on a plane-wave background.

To this end, let us analyze the properties of the multiple velocities. It is evident that the velocities ν_1 and ν_2 are real parameters, while the velocities μ_1 and μ_2 are real or complex depending on the value $m + 2\alpha$. Specifically, when $m + 2\alpha \geq 0$, μ_1 and μ_2 are real; and when $m+2\alpha < 0$, μ_1 and μ_2 are complex. As a result, a critical normalized frequency or a critical self-steepening parameter $S = -q - \sqrt{-2g + q^2}$ is extracted when $m+2\alpha = 0$, which leads to the transition between rogue waves and solitons. This finding is verified strictly by the modulation instability (MI) analysis where the marginal stability condition is consistent with the transition condition (see the following).

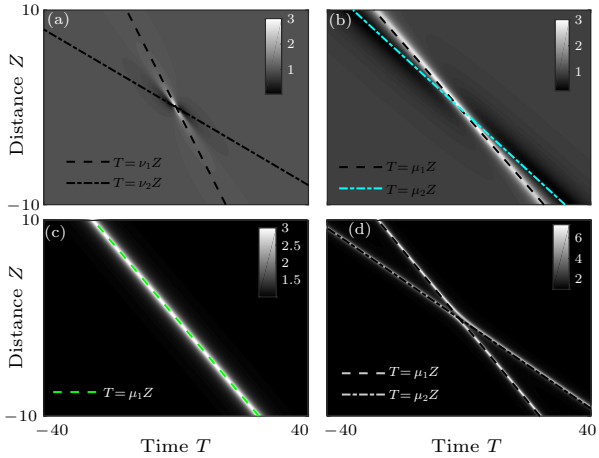

Fig. 2. Different types of localized waves in defocusing regime of NIMs as the self-steepening effect attenuates. From left to right, (a) rogue wave with $S = 1$, (b) antidark–dark soliton with $S = 0.56$, (c) antidark soliton with $S = 0.5$, and (d) antidark soliton pair with $S = 0.3$. The parameters are $g = 1$, $q = -2$ and $\tau_{\rm p}/\tau_{\rm opt} = 4$.

We first consider the case $\alpha < -m/2$. Thus only velocities ν_1 and ν_2 are valid. The intensity distribution of the localized waves with $S = 1$ is depicted well in Fig. 2. In this case, the expression (7) describes amplitude peaks which are localized in both z and t. This wave is the analogue of the Peregrine rogue wave with one peak and two valleys. Interestingly, both peak and valley of this rogue wave are tilted by the self-steepening effects. This is different from the known tilted rogue wave where only the peak is tilted.[18] Remarkably, the trajectories of the peak and valley can be described approximately by the lines $T = \nu_1 Z$ and $T = \nu_2 Z$, respectively.

If $\alpha \geq -m/2$, an interesting phase transition will occur. As shown in Fig. 2(b), the rogue wave is converted to an antidark–dark soliton pair with $\alpha = -m/2$. Namely, the longitudinal localization is broken completely. One can see that the peak of the rogue waves becomes elongated and eventually converts to an antidark soliton, while the valleys become

a dark soliton. The trajectory of the antidark–dark soliton pair can be described approximately by the lines $T = \mu_1 Z$ and $T = \mu_2 Z$, respectively. Note that the antidark–dark soliton pair exists with $\mu_1 \neq \mu_2$. Once $\mu_1 = \mu_2$, resulting in $\alpha = 0$, the solution describes a single pulse. The corresponding expression is given by

$$U(T, Z) = a\left[1 + \frac{4}{1 - 2im(T - \mu_1 Z)}\right]e^{i\theta}. \quad (10)$$

As shown in Fig. 2(c), the wave features a soliton structure on a plane-wave background which is known as the antidark soliton.

Next if $\alpha > 0$, the single antidark soliton will possess multiple velocities. As a result, the single antidark soliton is transited into an antidark soliton pair with propagation trajectories $T = \mu_1 Z$ and $T = \mu_2 Z$, as shown in Fig. 2(d).

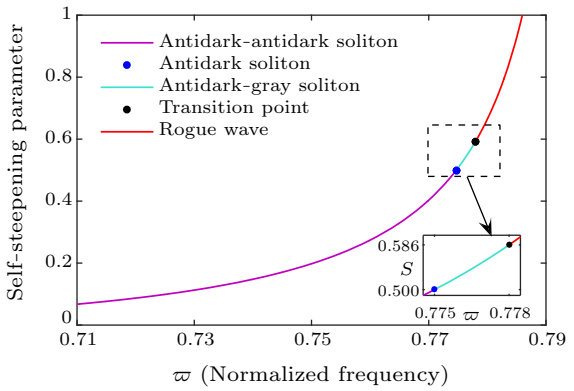

Fig. 3. (Color online) Phase diagram of different types of localized waves in the defocusing regime of NIMs in the (ϖ, S) plane.

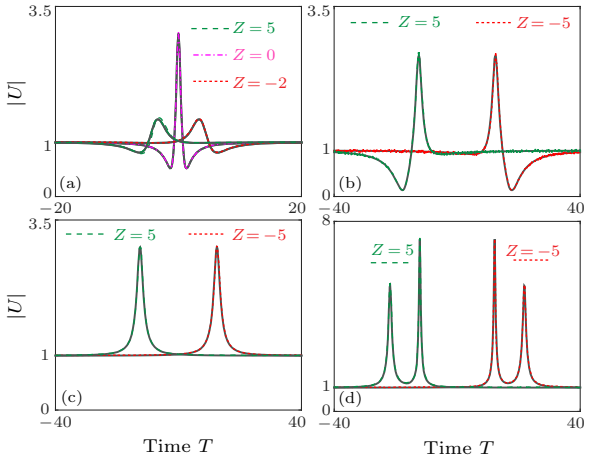

Fig. 4. Numerical stability confirmation of localized-wave excitations in Fig. 2 with the initial condition $U_{\rm in} = U(T, -10)[1 + 0.1\text{Random}(T)]$. The bottom shows the comparison of amplitude profiles of the analytical solution (black solid line) and the numerical results at different Z.

Based on the above analysis, we then plot the phase diagram of different types of localized waves in the defocusing regime of NIMs in the (ϖ, S) plane. The outline is depicted well in Fig. 3. As the self-steepening effect attenuates, the sequential transition that involves the rogue wave, antidark–dark soliton pair, antidark soliton and antidark soliton pair is triggered in the region $0.71 < \varpi < 0.8$. As shown in Fig. 3, the transition between rogue waves and soliton occurs when $\varpi = 0.778$. This result will provide a global overview of nonlinear waves on a plane-wave background in the defocusing regime of NIMs.

The propagation stability plays an important role in nonlinear wave realization and application. One should keep in mind that the solutions reported above are on a plane-wave background. The latter, in general, displays the feature of MI. Namely, the nonlinear waves on plane-wave background will be distorted and amplified.[28] Thus the numerical confirmation of the stability needs more exploration. Recent studies[22,24] demonstrated the stability of some types of nonlinear waves on a plane-wave background including the known rogue waves, W-shaped solitons, and the recently found multipeak solitons. Here we study numerically the stability of the nonlinear structures in the defocusing regime of negative-index metamaterials with the split-step Fourier method. The initial condition is given by the exact solution (9) at $Z = -10$ against white noise, i.e., $U_{\rm in} = U(T, -10)[1 + 0.1\text{Random}(T)]$. The corresponding numerical results are clearly shown in Fig. 4.

Interestingly, the numerical result shows clearly that the different types of nonlinear structures can propagate in a stable manner against the MI and ineradicable numerical deviations. In particular, we compare the numerical result with the analytical solution via the amplitude profiles at different Z. It shows in Fig. 4 that the numerical result (dotted line) is in good agreement with the analytical solution (solid black line) at different Z. These results confirm numerically the stability of different localized excitations on a plane-wave background, which could be useful for the corresponding experimental observation in the defocusing regime of negative-index metamaterials.

Let us investigate the transition mechanism of the localized waves reported above. To this end, we pay attention to the standard linear stability analysis of the plane wave U_0. A perturbed nonlinear background can be written as $U_{\rm p} = (a + \epsilon)e^{i\theta}$, where $\epsilon(Z, T)$ is a small perturbation which satisfies a linear equation. Generally, $\epsilon(Z, T)$ is given by collecting the Fourier modes as $\epsilon = f_+ e^{i(QT + \Omega Z)} + f_-^* e^{i(QT + \Omega^* Z)}$, where f_+ and f_- are small amplitudes, Q is the perturbed frequency, and the propagation parameter Ω is assumed to be complex. A substitution of the perturbed solution $U_{\rm p}$ into Eq. (9), followed by linearization and the process for the occurrence of baseband MI,[40] yields the dispersion relation

$$\Omega = -2(q + m) \pm \sqrt{Q^2 + m(m + 2\alpha)}. \quad (11)$$

MI exists when $\text{Im}\{\Omega\} \neq 0$, which implies $Q^2 +$

$m(m+2\alpha) < 0$. In general, MI is described by the growth rate $G = -\mathrm{Im}\{\Omega\}$. Namely, perturbations in this case suffer MI and grow exponentially as $\exp(Gz)$ at the expense of pump waves. Instead, MI is absent when $Q^2 + m(m+2\alpha) \geq 0$. In this case, the growth rate is vanishing ($G = 0$), which implies that the perturbation cannot be amplified.

It is generally recognized that MI is among the several mechanisms that generate rogue waves. In particular, recent studies[40,41] demonstrate that rogue waves exist in the vanishing frequency perturbation regime of MI, i.e., $\mathrm{Im}\{\Omega\}|_{Q=0}$. Thus one can verify that the rogue waves in Eq. (4) exist in the region $m + 2\alpha < 0$, which is consistent with the existence condition of rogue waves obtained from the exact solution. In particular, the marginal stability condition $\mathrm{Im}\{\Omega\}|_{Q=0} = 0$ coincides with that of the transition between rogue waves and solitons.

In Fig. 5, we depict the characteristic of MI growth rate in the (ϖ, Q) plane. It shows clearly that the marginal stability condition ($\varpi = 0.778$) is consistent with the condition of the transition between rogue waves and solitons, as shown in Fig. 3. Our result demonstrates that the transition of rogue waves and solitons occurs as a result of the attenuation of MI growth rate to vanishing in the zero-frequency perturbation region.

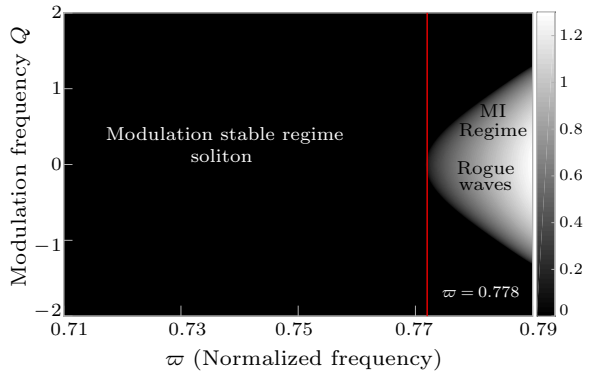

Fig. 5. (Color online) Characteristic of MI growth rate in the (ϖ, Q) plane. The setup is the same as in Fig. 2.

Finally, we discuss the difference between the self-focusing case and the self-defocusing case regarding the transition of localized waves related to localized waves in the NIMs. It is found that the focusing regime also supports the transition between rogue waves and soliton with a larger value of self-steepening parameter $S(> 4.45)$ for a fixed background frequency q ($q = -2$ in Fig. 2). However, for ultrashort pulse propagation in NIMs governed by the higher-order NLSE, the self-steepening effect should be a small value ($S < 1$) compared with the values of second-order dispersion and cubic nonlinearity.[6,35] As a result, in the case of $S < 1$ we find that the transition between rogue waves and solitons in the focusing regime of NIMs vanishes. Namely, only rogue waves exist in the focusing regime of NIMs. It comes from the fact that in this case the MI always exists in the zero-frequency perturbation region.

In summary, we have studied localized waves on a plane-wave background in the defocusing regime of NIMs with self-steepening effect. Important characteristics of localized waves, such as the transitions, propagation stability, and mechanism, are revealed in detail. We demonstrate that the sequential transition that involves the rogue wave, antidark–dark soliton pair, antidark soliton and antidark soliton pair can be triggered as the self-steepening effect attenuates. In particular, our results demonstrate that transition between rogue waves and solitons occurs as a result of the attenuation of MI growth rate to vanishing in the zero-frequency perturbation region.

References

[1] Veselago V G 1968 *Sov. Phys. Usp* **10** 509
[2] Kapitanova P V et al 2011 *Appl. Phys. Lett.* **99** 251914
[3] Shadrivov I V et al 2012 *Phys. Rev. Lett.* **109** 083902
[4] Smith D R et al 2000 *Phys. Rev. Lett.* **84** 4184
[5] Shelby R A et al 2001 *Science* **292** 77
[6] Zharov A A et al 2003 *Phys. Rev. Lett.* **91** 037401
[7] Pendry J B et al 2006 *Science* **312** 1780
Shalaev V M 2007 *Nat. Photon.* **1** 41
[8] Tlidi M et al 2011 *Phys. Rev.* A **84** 013807
[9] Zhang L et al 2015 *Appl. Phys.* B **121** 465
[10] Wang Y F et al 2015 *Phys. Rev.* B **92** 104110
[11] Gabitov I R et al 2006 *J. Opt. Soc. Am.* B **23** 535
[12] Wang Z et al 2010 *J. Appl. Phys.* **107** 094907
[13] Scalora M et al 2005 *Phys. Rev. Lett.* **95** 013902
[14] Biswas A et al 2014 *Optik* **125** 3299
Biswas A et al 2014 *J. Mod. Opt.* **61** 1550
[15] Boardman A D et al 2010 *Opt. Commun.* **283** 1585
[16] Xu Y et al 2016 *Opt. Laser Technol.* **77** 177
[17] Li P 2010 *Phys. Rev.* E **82** 046603
[18] Kibler B et al 2010 *Nat. Phys.* **6** 790
[19] Akhmediev N et al 2009 *Phys. Rev.* E **80** 026601
[20] He J et al 2014 *Chin. Phys. Lett.* **31** 010502
He J et al 2015 *AIP Adv.* **5** 017105
[21] Ren Y et al 2015 *Phys. Lett.* A **379** 2991
Ren Y et al 2016 *Eur. Phys. J.* D **70** 187
[22] Liu C et al 2015 *Phys. Rev.* E **91** 022904
[23] Liu C et al 2015 *Ann. Phys.* **362** 130
[24] Liu C et al 2016 *Phys. Rev.* E **94** 042221
[25] Chowdury A et al 2015 *Proc. R. Soc.* A **471** 20150130
[26] Wang L et al 2016 *Phys. Rev.* E **93** 012214
[27] Zakharov V E et al 2009 *Physica* D **238** 540
Zakharov V E et al 2013 *Phys. Rev. Lett.* **111** 054101
[28] Dudley J M et al 2014 *Nat. Photon.* **8** 755
[29] Solli D R et al 2007 *Nature* **450** 1054
[30] Liu C et al 2014 *Phys. Rev.* A **89** 055803
[31] Liu C et al 2014 *Opt. Lett.* **39** 1057
Duan L et al 2016 *Chin. Phys. Lett.* **33** 010501
[32] Wang X et al 2014 *Chin. Phys. Lett.* **31** 090201
[33] Shen Y et al 2017 *Phys. Rev.* E **95** 032223
[34] Essama B G O et al 2014 *Phys. Rev.* E **90** 032911
Essama B G O et al 2014 *Opt. Commun.* **331** 334
[35] Wen S et al 2006 *Opt. Express* **14** 1568
[36] Wen S et al 2007 *Phys. Rev.* A **75** 033815
[37] Wen S et al 2006 *Phys. Rev.* E **73** 036617
Xiang Y et al 2010 *Phys. Rev.* E **82** 056605
[38] Sarmaa A K 2011 *Eur. Phys. J.* D **62** 421
[39] Guo B L et al 2012 *Phys. Rev.* E **85** 026607
Guo B L et al 2014 *Phys. Rev.* E **89** 041201
[40] Baronio F et al 2014 *Phys. Rev. Lett.* **113** 034101
[41] Zhao L C and Ling L M 2016 *J. Opt. Soc. Am.* B **33** 850